





## BIO-WASTE-BASED CEMENT FOR SUSTAINABLE CIVIL ENGINEERING PRACTICE CEMENT ZASNOVAN NA BIO-OTPADU ZA ODRŽIVU GRAĐEVINSKU PRAKSU


Originalni naučni rad / Original scientific paper  
Rad primljen / Paper received: 01.11.2024  
<https://doi.org/10.69644/ivk-2024-03-0283>

Adresa autora / Author's address:

<sup>1)</sup> Institute for Testing of Materials, Belgrade, Serbia A. Terzić  0000-0002-4762-7404; N. Mijatović  0000-0002-1751-6498; K.

Janković  0000-0003-3744-3799; D. Bojović  0000-0002-4900-6177 \*email: [anja.terzic@institutims.rs](mailto:anja.terzic@institutims.rs)

<sup>2)</sup> Institute of Technical Sciences of the SASA, Belgrade, Serbia S. Filipović  0000-0001-6383-8327; N. Obradović  0000-0002-7993-293X

<sup>3)</sup> Missouri University of Science and Technology, Parker Hall, Rolla, MO, USA W.G. Fahrenholtz  0000-0002-8497-0092

### Keywords

- eggshell waste
- mechanical activation
- thermal treatment
- microscopy
- building materials

### Abstract

*Industrial byproducts are being increasingly used as raw materials in the cement clinker production. This can help to address the issue of huge amounts of eggshell waste that are discarded into the environment. This bio-waste has a trigonal-calcite structure and similar behaviour as limestone. In this study, cement clinker is synthesized at 1300 °C using eggshell waste in place of limestone. The raw materials are mechanically activated in a high-energy mill. The sintering kinetics are calculated using the results of differential thermal analysis. Mechanical activation modified the spatial distribution of Al, Si, Ca, and Fe, thereby improving the reactivity which in turn decreased the sintering temperature of the clinker. The study demonstrated that eggshell waste is a suitable replacement for limestone in the production of ordinary Portland cement.*

### INTRODUCTION

Given the rapid rise in construction and infrastructure works, the need for cement-based products has led to a significant environmental impact through the manufacturing of building materials. The beneficial characteristics of ordinary Portland cement (OPC) include good workability, quick setting, rapid hardening, superior mechanical properties, and appropriate chemical resistance /1/. For these reasons, OPC has been the primary binder in the building industry for over 200 years. OPC is generally employed along with aggregates and water to produce concrete or mortar. The cement solidifies through a complex hydration process to provide the necessary strength for structural elements or construction, /2-4/. The manufacturing of cement surged significantly in the 2000s, amounting to 4000 million tons in the preceding ten years. Cement production and consumption accounts for 8 % of the global CO<sub>2</sub> emissions, /5-8/. From the overall total, the production of clinker accounts for 50 % of the carbon emissions, fuel combustion for 40 %, and transportation, raw material processing, drying, crushing, and blending for 10 %, /9/. Cement consumption is unlikely to decrease in the near future due to the availability of the

### Ključne reči

- otpad ljsuske jajeta
- mehaničko aktiviranje
- termička obrada
- mikroskopija
- građevinski materijali

### Izvod

*Industrijski nusproizvodi se sve više koriste kao sirovine u proizvodnji cementnog klinkera. Ovo može pomoći da se reši problem ogromnih količina bio-otpada (na pr. ljsuske od jaja) koji se odlaze u životnu sredinu. Ovaj biootpad ima trigonalno-kalcitnu strukturu i karakteristike slične krečnjaku. U ovoj studiji, cementni klinker je sintetizovan na 1300 °C koristeći biootpad umesto krečnjaka. Sirovine su mehanički aktivirane u visokoenergetskom mlinu. Kinetika sinterovanja je izračunata na osnovu rezultata diferencijalne termičke analize. Mehanička aktivacija je modifikovala prostornu distribuciju Al, Si, Ca i Fe, čime je poboljšana reaktivnost, što je zauzvrat smanjilo temperaturu sinterovanja klinkera. Studija je pokazala da je otpad od ljsuske jajeta pogodna zamena za krečnjak u proizvodnji običnog portland cementa.*

natural resources needed for its production and the ongoing large-scale construction projects taking place all over the world. For every kilogram of cement produced, an estimated 0.9 kg of CO<sub>2</sub> is released, with the calcination and combustion processes contributing to more than 90 % of the total CO<sub>2</sub> emissions, /10, 11/. The predominance of non-renewable resources in cement manufacturing has given rise to significant environmental concerns. Consequently, researchers and industry professionals are developing creative solutions to deal with these growing issues.

Commercial manufacturing of OPC involves calcinating the raw materials in a rotating kiln. Rotary kilns are not energy-efficient, but research is in progress to make this process less energy-demanding, improve the ability to use diverse energy resources, and increase environmental friendliness, /12, 13/. Principal components of OPC are limestone, quartz, clay, and slag (e.g., blast furnace slag or similar Fe-bearing slag); however, various industrial wastes have occasionally been used to produce cement clinker. A current research trend in the cement industry is recycling waste materials to reduce industrial byproducts from landfills. Numerous studies on the reuse of industrial waste as an

alternative for OPC raw materials have been conducted in response to the growing social demand for sustainability and circularity. The cement industry has also made major efforts in this direction, /14-17/. A cautious approach has been taken to the resources used in the production of cement clinker since alternative raw materials also need to be accessible in adequate quantities and of acceptable quality.

Numerous attempts were made to find substitutions for cement or raw materials for cement production. Reusing waste materials could reduce the amount of cement used and the harm that open waste disposals impose on the environment, /18-20/. For example, reusing fine sediment waste from hydroelectric dams that contain Si- and Al-based minerals for cement clinker is a viable option, /21/. Research was also conducted on waste materials that include quartz /22/, concrete and ceramic waste /23/, red mud /24/, and coal combustion fly ash (FA) /25/. Iron ore tailings /26/ and crushed steel slag /27/ have also been employed in the production of cement clinker. Comparatively less research, however, has been done on substitutes for limestone as a raw material in cement production, /28-30/. Agriculture residues are among the solid wastes that can be reused in the building industry. Recent research has employed these byproducts as a partial cement replacement. Ash from rice husks /31/, sawdust ash /32/, sugar cane bagasse /33/, and oyster shell ash /34/, have all been investigated as cement substitutes. Even though standard industrial byproducts such as fly ash show outstanding structural performance, using bio-based wastes provides advantages such as being readily accessible, economical, lightweight, recyclable, energy-efficient, and environmentally acceptable.

One example of bio-based waste for which a suitable recycling treatment method has not yet been proposed is the protective shell that surrounds eggs. Global egg production is increasing, and it is estimated that 8 million tons of waste eggshells (ES) will be produced yearly. ES are discarded in large amounts despite the fact that they can be used to make calcium phosphate ceramics, as a biofuel feedstock, as an extractor for ionic contaminants, and as fertilizer, /35/. The primary component of ES is  $\text{CaCO}_3$ , which makes up 96-97 % of the total weight. Membranes and other organic components make up the final 3.4-5 % weight. Trigonal calcite is the calcium carbonate structure found in eggshells and is the same as that of limestone, which is an essential mineralogical component of OPC binder, /36/. Therefore, dry powder calcium carbonate can be used as a cement alternative in building materials.

Using ES powder in various construction materials helps mitigate environmental issues due to the direct recycling of this bio-waste /37-39/. ES powder has been assessed for use in sustainable, cost-effective construction as cement pastes, mortars, concrete, soil stabilizers, and sandcrete blocks /40, 41/. Physical, chemical, morphological, and mineralogical characteristics of powdered ES are different from those of cement particles, /41/. For instance, cement with a high volume of fly ash (HVFA) was partially replaced with ES to improve the subpar performance of concrete containing FA. The ES is used as a source of calcium carbonate, which was then utilized to accelerate the hydration of FA cement.

When  $\text{CaCO}_3$  from ES was introduced to the HVFA cementitious matrix, the carbonate ion and the aluminate hydrate from Portland cement hydration interacted to produce carboaluminates, /42/. Thereby, the addition of  $\text{CaCO}_3$  from ES aided in the development of ettringite and mono-carbonate, which improved the mechanical strengths of the resulting concrete, /43/. In the work of Binici et al. /44/, powdered ES is used as a physical shield to insulate structures from radiation damage because ES concrete has lower radioactive permeability. Fine sand fractions are replaced with ground ES, and the strengths are tested after 7, 28, and 90 days. The development of strength is delayed as the ES additive ratio increased. Pliya and Cree /45/ compared the natural limestone with the efficacy of pulverized ES waste in cement mortar as an OPC substitute. Due to the filler's influence on the microstructure, replacing part of the cement with limestone increased strength development in the mortar; nevertheless, mortar prepared with ES cement had inferior mechanical properties at all replacement ratios. Zain et al. /46/ investigated the rheological and mechanical properties of self-compacting concrete (SCC) containing 0.6  $\mu\text{m}$  eggshell particles as a partial replacement for cement. Sieve segregation tests, L-box, and slump flow were utilized to assess the properties of the concrete mixture. Compressive and flexural strengths were evaluated at 28 days. Theoretical values were compared with the final flexural strength and fracture length of the SCC beams. The flexural strength of ES-containing SCC beams was comparable to that of Eurocode 2, while the fracture length was smaller than the permitted value in Eurocode 2.

Very few reports have been made on the use of ES waste in the production of cement clinker up to this point, /47/. The goal of this study is to produce cement clinker based on pulverized eggshell waste as a substitution for limestone. The eggshell cement clinkers (ESC) were synthesized under identical conditions (high energy milling for 10, 20, and 30 minutes, and subsequent sintering at 1300 °C). All ESC clinkers included pulverized eggshells, Fe-slag, and quartz. The fourth component of the clinker varied: clay, zeolite, bentonite, or fly ash. Outputs of mechanical activations were compared using specific surface area analysis and scanning electron microscopy (SEM) accompanied by energy dispersive X-ray spectroscopy (EDS) for targeted analysis of sample surfaces. The kinetics of sintering were assessed using the results of differential thermal analysis. The obtained results confirmed the feasibility of manufacturing bio-waste-based cement.

## EXPERIMENTAL PROCEDURE

### *Characterisation of materials and mix design of cement clinkers*

Five different cement clinkers are prepared. The mix design and labels are given as diagrams in Fig. 1. Eggshell cement clinkers (ESC) contained eggshell (ES) as a substitute for limestone (i.e., calcium carbonate), quartz sand (pure  $\text{SiO}_2$ ), alumino-silicate mineral bearer (clay from *Zaječar* deposit; zeolite from *Vranjska banja* deposit, bentonite from *Šipovo* deposit, and fly ash from Kolubara power plant) /48, 49/, and Fe-slag. Limestone cement clinker (LSC) was pre-

pared using limestone /50/, quartz sand, clay, and Fe-slag. The Fe-slag contained 51.19 wt.% of iron. Mix design and labels of experimental mixtures for production of cement clinkers are given in Fig. 1.

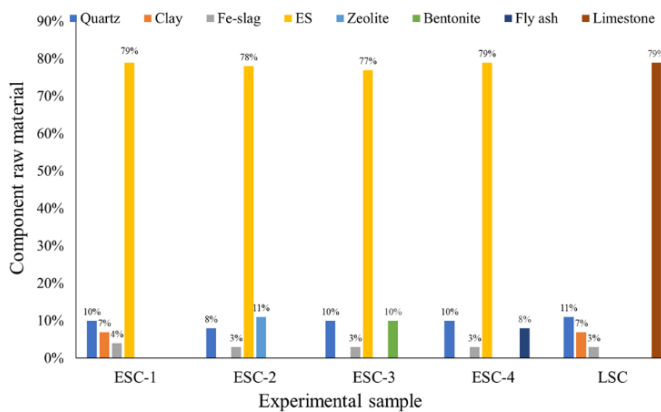


Figure 1. Mix design and labels of experimental mixtures for production of cement clinkers.

Raw materials are dried at 105 °C in a laboratory dryer before pulverization in a Herzog vibratory disc mill. Pulverized samples ( $d_{50} < 63 \mu\text{m}$ ) are used for chemical analyses. Identification and quantification of major oxides was conducted by energy dispersive X-ray fluorescence method (Spectro Xepos, SPECTRO Analytical Instruments) equipped with a 50 W and 60 V X-ray tube with a binary Co/Pd alloy target anode. The excitation mode of the X-ray tube utilized polarized/direct excitation. The characteristic radiation emitted by the elements present in the sample was collected by a silicon drift detector with a Peltier cooling system. Loss on ignition (LoI) was measured at 1000 °C using laboratory furnace.

#### Mechanical activation of mixtures for cement clinkers

Mixed raw materials were activated by means of the laboratory high energy ball mill (SPEX D8000, SPEX Certi-Prep). Dry high-energy ball milling was conducted using tungsten carbide (WC) milling media and jar for 10, 20, and 30 minutes in an air atmosphere. All milled powders (ESC1-4 and LSC) were sieved through a 60-mesh sieve. Contamination from WC media was estimated by measuring the mass of the media before and after milling and was below 1 wt.%.

Specific surface area of the mechanically activated samples was determined using the Brunauer-Emmett-Teller (BET) method. A physisorption BET surface area analyser (Nova 600 BET, Anton Paar) was used. The analysis gas was  $\text{N}_2$  with a relative pressure range ( $P/P_0$ ) from  $10^{-4}$  to 0.5. Powders were degassed in vacuum for three hours at 100 °C prior to analysis.

Scanning electron microscopy (eLine Plus, Raith) accompanied by energy dispersive X-ray spectroscopy (QUANTAX, Bruker) for targeted analysis of sample surfaces were performed on mechanically activated powders.

#### Sintering of mixtures for cement clinkers

The samples ESC-1-4 and LSC were sintered in a laboratory chamber furnace at a maximal temperature of 1300 °C. Pressed pellets were heated at 10 °C/min to 800 °C with a one hour hold at that temperature. Then, the pellets were

heated at 10 °C to 1300 °C and held for two hours, following which the furnace was turned off.

Powder mixtures were subjected to differential thermal analysis (SETSYS TG/DTA/DSC, SETARAM Instrumentation). Samples (30 g) were placed in an alumina pan and heated from 20 °C to 1000 °C. Heating rates were 10, 20, and 30 °C/min. The analysis was performed in a static air. The Kissinger approach, based on how the position of peak maxima changes as the heating rate increases, was used to analyse kinetics /55-54/. The following equation illustrates how reaction rate varies with temperature, /51-54/:

$$\frac{d\alpha}{dt} = f(\alpha) \times k(T), \quad (1)$$

where:  $\alpha$  is the reaction's extent;  $f(\alpha)$  is a function of the reaction mechanism; and  $k(T)$  is the rate constant at temperature  $T$ . The  $k(T)$  has Arrhenius equation form:

$$k(T) = A e^{-\frac{E_a}{RT}}, \quad (2)$$

where:  $A$  ( $\text{min}^{-1}$ ) is the pre-exponential factor or frequency factor (theoretical value is  $A = 1 \times 10^5 \text{ s}^{-1}$ );  $E_a$  ( $\text{kJ} \cdot \text{mol}^{-1}$ ) is the apparent activation energy of the transformation;  $R$  is ideal gas constant ( $R = 8.314 \text{ kJ} \cdot \text{mol}^{-1} \text{ K}^{-1}$ ); and  $T$  (K) is absolute temperature.

The general rate equation is typically formulated by combining the Arrhenius equation, Eq.(2), and the reaction rate Eq.(1), /51-54/:

$$\frac{d\alpha}{dt} = A \times f(\alpha) e^{-\frac{E_a}{RT}}. \quad (3)$$

A final form of Kissinger equation is derived by performing diffraction by sections of Eq.(3) and other transformations as described in other studies, /51-54/:

$$\ln\left(\frac{\beta}{T_p^2}\right) = \ln\left(\frac{A \times R}{E_a}\right) - \frac{E_a}{R \times T_p}, \quad (4)$$

where:  $\beta$  is a constant heating rate  $dT/dt$  ( $\text{Kmin}^{-1}$ ); and  $T_p$  (K) is maximal absolute temperature at which the reaction maximum occurs.

Varying the rate of heating results in different peak temperatures. Linear regression analysis of  $\ln(\beta/T_p^2)$  versus  $1/(R \times T_p)$  can then be used to compute the activation energy. Namely, in this plot, the data points lie on a straight line whose slope represents activation energy  $E_a$  of the process.

## RESULTS AND DISCUSSION

The chemical analyses of ESC1-4 and LSC powder mixtures are provided in Fig. 2.

Figure 3 shows the change of specific surface area (SSA) values with the duration of mechanical activation. The highest increase in SSA for the ESC powders was seen after 10 minutes of activation. The SSA increased by about 55 % for all ESC mixtures for 10 minutes of activation. When the activation period was raised from 10 to 20 minutes, the difference in SSA was around 20 %, and it was roughly 15 % when the time was prolonged to 30 minutes. Among the ESC mixtures, ESC-4 (fly ash) consistently exhibited the highest SSA values, followed by ESC-2 (zeolite). The LSC sample demonstrated different behaviour. Following an initial increase in SSA of approximately 60 % after 10 minutes of

activation, increments for 20 and 30 minutes of activation were just 1-2 %. As a result, eggshell-based mixtures were more easily activated than conventional limestone cement clinker blends. Because the eggshell-based clinker mixtures have higher SSA, they should be more reactive due to the smaller mean particle size that will increase the number of contacts with other particles.

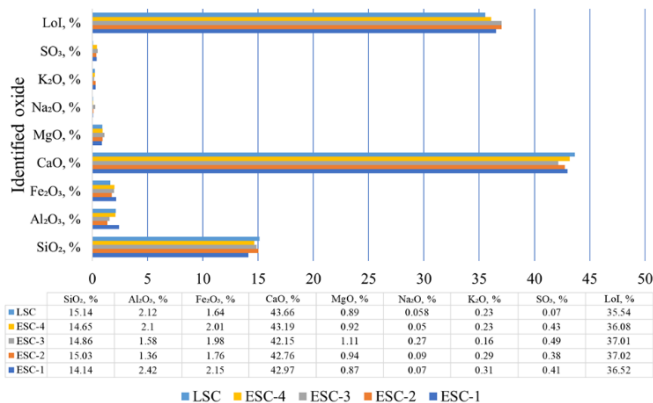


Figure 2. Chemical composition of experimental mixtures for production of cement clinkers.

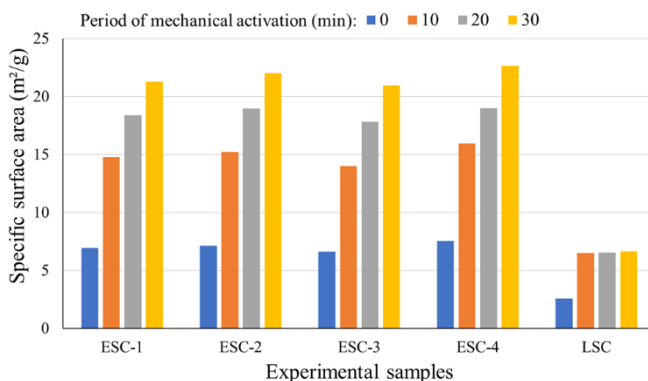


Figure 3. Specific surface area of experimental mixtures for production of cement clinkers.

Figures 4-8 give a preview of SEM analysis of the starting (untreated) and mechanically activated clinker mixes. Microphotographs are taken at 7500× magnification and EHT = 10.00 kV.

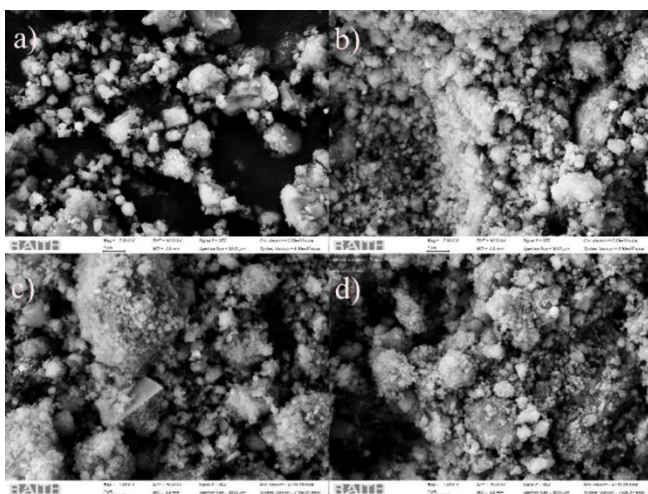


Figure 4. SEM micrographs of ESC-1 activated for: a) 0 min; b) 10 min; c) 20 min, and d) 30 min.

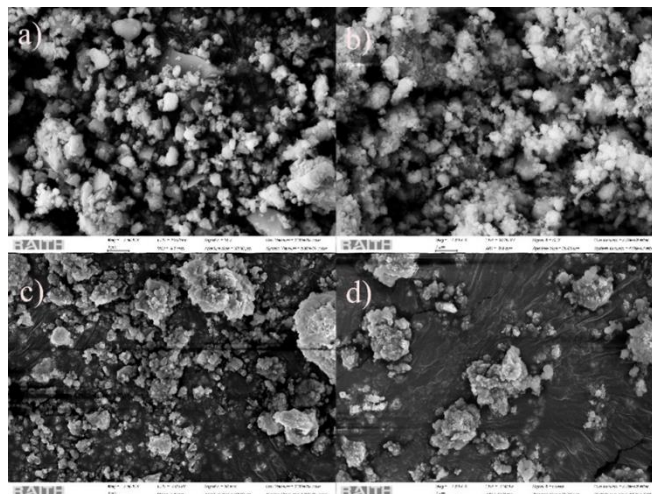


Figure 5. SEM micrographs of ESC-2 activated for: a) 0 min; b) 10 min; c) 20 min, and d) 30 min.

ESC-1 is composed of clay, eggshell powder, Fe-slag, and quartz. As can be seen in the microphotograph of the initial sample (Fig. 4a), the majority of the particles are submicron. Quartz particles are typically larger (1.5-2 μm in diameter). Figure 4b shows ESC-1 after 10 minutes of mechanical activation. Nearly all of the particles are submicron in size with very few apparent agglomerates. Figures 4c and 4d show ESC-1 samples after 20 and 30 minutes of activation. The clay particles formed agglomerates in both powders. According to microphotography and visual observation, a 10-min activation period is suitable for the ESC-1 sample based on apparent particle size reduction, but minimal agglomeration.

Figure 5 shows ESC-2 that consists of eggshell powder, zeolite, Fe-slag, and quartz. Figure 5a shows prismatic and rhombohedral particles that range in size from micron down to submicron sizes. Quartz has larger grains, while zeolite particles are less than 1 μm in diameter. Figure 5c illustrates an ESC-2 mixture mechanically activated for 20 minutes, which has a mixture of individual grains and agglomerates. Mechanical activation for 30 minutes resulted in the highest degree of agglomeration, as shown in Fig. 5d.

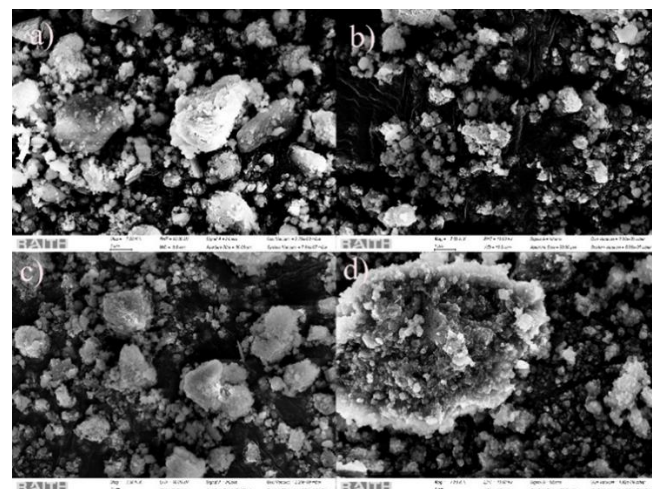


Figure 6. SEM micrographs of ESC-3 activated for: a) 0 min; b) 10 min; c) 20 min, and d) 30 min.

ESC-3 is composed of eggshell powder, bentonite, Fe-slag, and quartz. After 10 minutes of mechanical activation (as shown in Fig. 6b) the agglomeration process began, but some individual particles are also present. The size and number of agglomerates appeared to increase after 20 minutes of milling as shown in Fig. 6c. After 30 minutes of milling, most of the particles gathered into a single, massive structure (Fig. 6d).

The activation of a cement clinker mixture containing fly ash (ESC-4) produced the best results after 10 and 20 min of mechanical treatment. Figures 7b and 7c illustrate grain mixes made up primarily of micron and submicron-sized grains. In contrast to grains in Fig. 7d, the particles visible in Figs. 7b and 7c have not yet fused into larger forms.

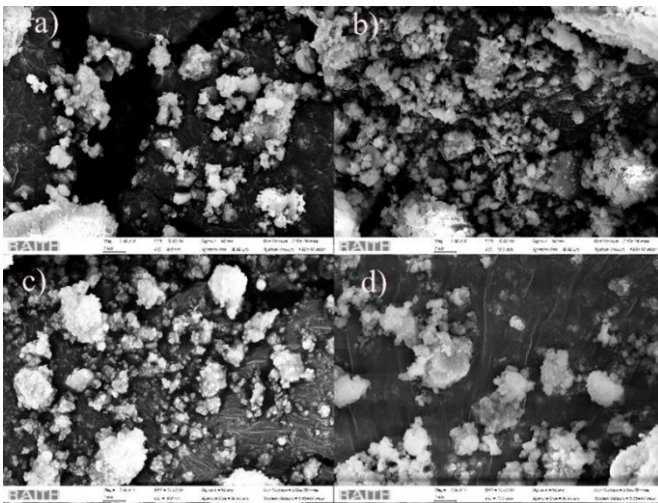


Figure 7. SEM micrographs of ESC-4 activated for: a) 0 min; b) 10 min; c) 20 min, and d) 30 min.

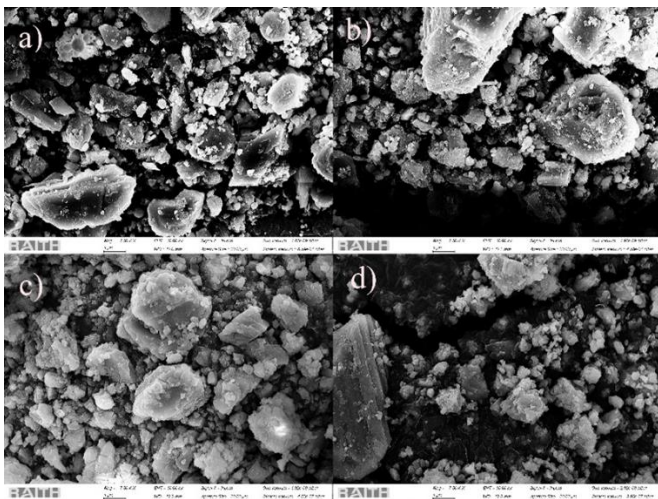


Figure 8. SEM micrographs of LSC activated for: a) 0 min; b) 10 min; c) 20 min, and d) 30 min.

Limestone is the most abundant component of the LSC powders because it makes up about 79 wt.% of the composition. Although the overall chemical composition is similar to the ESC composition, the activation behaviour is substantially different. Specifically, the ESC compositions all exhibited a significant rise in SSA that corresponded to a clearly observable decrease in particle sizes during milling.

In contrast, the LSC mixture was not readily pulverized. The mean grain size of the mixture was reduced with the mean grain size decreasing threefold after 10 minutes of mechanical treatment. Agglomerates formed at the same time as the particle size reduction (as shown in Fig. 8b). The presence of agglomerates most likely influenced the minimal change in SSA seen during subsequent milling. Figures 8a-d show characteristic calcite crystals, which have prismatic and rhombohedral shapes. These grains are quite similar to those of calcite derived from pulverized eggshells. However, mechanical activation was more effective on the eggshell powder than typical limestone.

The spatial distribution of elements (Al, Ca, Si, and Fe) on the grains of untreated and mechanically treated samples was examined using EDS. Figures 9 and 10 show a targeted analysis of ESC-4 samples surfaces that were mechanically untreated (Fig. 9) and activated for 20 minutes (Fig. 10).

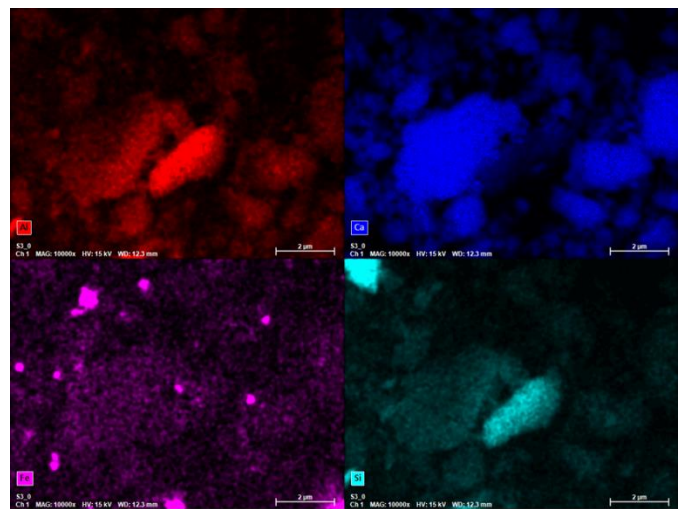


Figure 9. Spatial disposition of elements on grains of untreated ESC-4 sample.

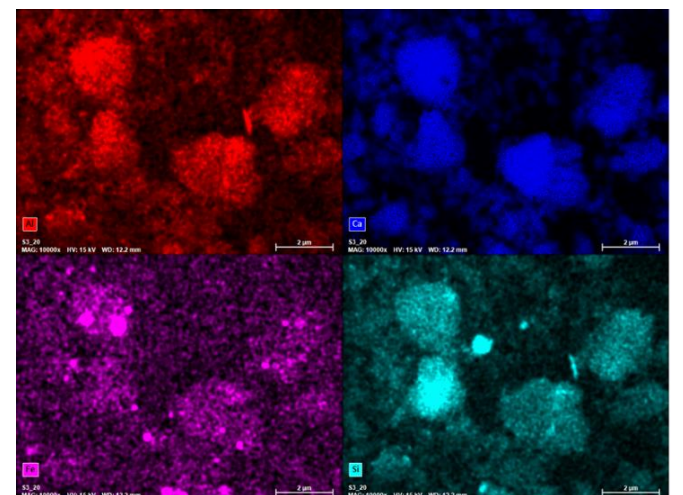


Figure 10. Spatial disposition of elements on grains of ESC-4 sample, mechanically treated for 20 min.

As represented by the area for each element shown in Figs. 9 and 10, Ca is the most abundant element, followed by Al and Si. Fe is quantitatively less abundant. Aside from lowering the mean grain size of the clinker mixture, mechan-

ical activation improved the distribution of the detected elements (Al, Si, Ca, and Fe). This is particularly apparent in the case of elemental iron. A wider and more dispersed distribution of reactive chemical elements on the grains in the mixture will contribute to the improved reactivity of the clinker during thermal treatment.

Figures 11 and 12 show elemental targeted analysis of the surfaces of LSC samples that were untreated (Fig. 11) and mechanically treated for 20 minutes (Fig. 12).

Figures 11 and 12 show elemental targeted analysis of the surfaces of LSC samples that have been mechanically untreated and then treated for 20 minutes. As previously stated, mechanical activation did not contribute to a considerable reduction in grain size of the LSC mixture. However, it improved the arrangement of elements on the surface of the grains and thereby influenced increase in the reactivity of the LSC clinker mixture.

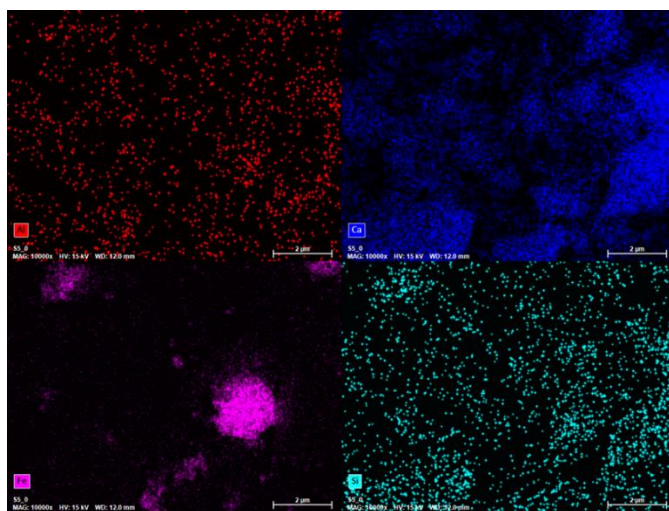


Figure 11. Spatial disposition of elements on grains of untreated LSC sample.

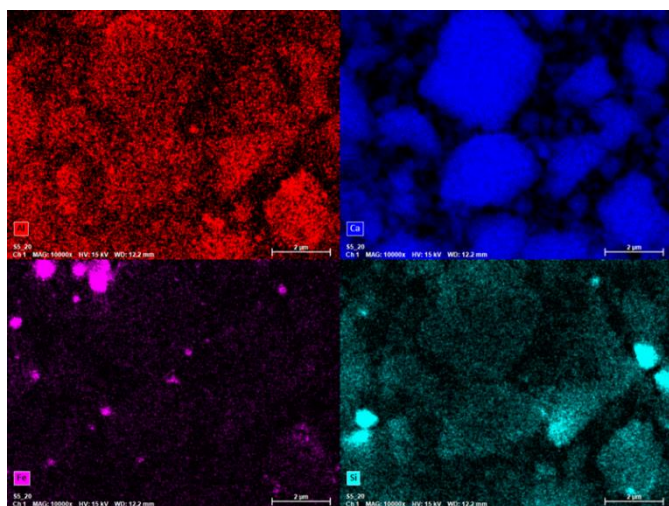


Figure 12. Spatial disposition of elements on grains of LSC sample, mechanically treated for 20 min.

Figure 13 shows DTA curves for ESC-4 recorded using different heating rates. The plot in Fig. 14 shows three main peaks ( $T_1$ ,  $T_2$ , and  $T_3$ ) plus a broad endothermic peak between 90 and 130 °C. The initial endothermic feature

between 90 °C and 130 °C was attributed to physical water evaporation and was not used in further calculations. The initial peak for ESC-4 sample was recorded at  $T_1 = 410.5$  °C at a heating rate of 10 °C per minute. Using faster heating rates, the peaks shifted to higher temperatures: 412.7 °C for 20 °C/min and 420.3 °C for 30 °C/min. The shift was slight for heating rates of 10 °C/min and 20 °C/min, amounting to only about 2 °C. The  $T_1$  peak appeared at a higher temperature when recording was conducted at a 30 °C/min rate. The initial peak ( $T_1$ ) corresponds to decomposition temperature of  $\text{Ca(OH)}_2$  /55/. The second endothermic effect ( $T_2$ ) was detected at 582.5 °C when the sample was heated at a rate of 10 °C per minute. This effect, detected while recording with faster heating rates, was set for higher temperatures, i.e., 590.6 °C and 603.8 °C, respectively. The second endothermic peak can be associated with a weight loss that takes place between 400 °C and 600 °C. The peak  $T_2$  is attributed to decomposition of boehmite ( $\gamma\text{-AlOOH}$ ) in aluminous materials such as clay, fly ash, zeolite, and bentonite, /56/. The third endothermic peak ( $T_3$ ) is found at 805.2 °C (at a heating rate of 10 °C/min). The associated maxima ( $T_3$ ) for 20 and 30 °C/min heating rates were 846.8 °C and 873.4 °C, respectively. This effect is associated with the decomposition temperature of  $\text{CaCO}_3$  and for the provision of CaO for the following solid phase reactions, i.e., it can be correlated with decomposition of limestone and eggshell /55, 56/. The very small effects from 950 °C onward are consistent with the temperature for forming the liquid phase (normally from 1295 °C to 1306 °C). This is the stage when complex solid-phase reaction processes are taking place, resulting in the formation of  $\text{C}_3\text{S}$  in the crystal phase of clinker, as well as anhydrous calcium sulfoaluminate ( $\text{C}_4\text{A}_3\text{S}$ ), dicalcium silicate ( $\text{C}_2\text{S}$ ), and brownmillerite ( $\text{C}_4\text{AF}$ ), /56/.

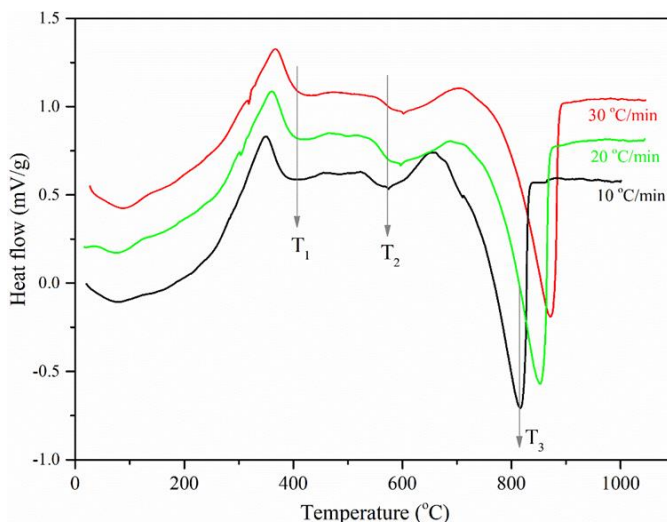


Figure 13. DTA curves of ESC-4 recorded using different heating rates.

Key temperature points of endothermic peaks in DTA curves are provided in Table 1.

Activation energies for sintering of cement clinker mixes are calculated using the Kissinger equations, Eqs.(1-4). The plots, i.e., linear regressions of  $\ln(\beta/T_p^2)$  versus  $1/(RT_p)$  and the obtained results are provided in Fig. 14 and Table 2, respectively. Activation energies were found to depend on

the surface area and reactivity of the powders as well as on the type of raw materials included in the sintering.

Table 1. Key temperature points of peaks in DTA curves.

Temp. (°C)	T <sub>1</sub>			T <sub>2</sub>			T <sub>3</sub>		
Heat. rate (°C/min)	10	20	30	10	20	30	10	20	30
	Sample								
ESC-1	410.2	415.7	420.1	580.5	585.6	607.9	800.3	805.4	810.7
ESC-2	415.2	420.6	423.8	597.2	581.4	599.5	813.7	820.4	827.3
ESC-3	407.3	409.5	418.7	570.5	579.7	588.3	802.6	812.5	826.7
ESC-4	410.5	412.7	420.3	582.5	590.6	603.8	805.2	846.8	873.4
LSC	380.1	383.4	384.7	563.8	570.1	590.2	860.1	867.4	870.2

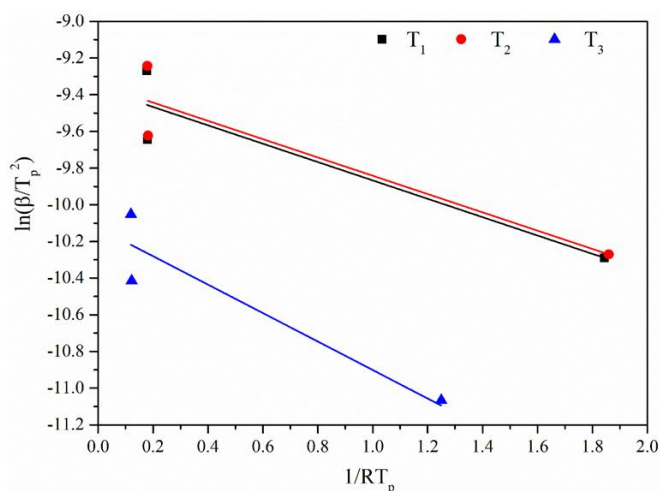


Figure 14. Activation energies for processes occurring at temperatures T<sub>1</sub>, T<sub>2</sub>, and T<sub>3</sub> in ESC-4 sample.

Table 2. Activation energies for processes marked with T<sub>1</sub>, T<sub>2</sub>, and T<sub>3</sub> in ESC-4 sample.

Process	T <sub>1</sub>	T <sub>2</sub>	T <sub>3</sub>
Sample	Activation energy (kJ/mol)		
ESC-1	118.14	135.87	175.35
ESC-2	119.20	133.25	173.96
ESC-3	121.30	139.15	183.75
ESC-4	117.25	132.51	170.39
LSC	189.24	205.95	229.36

Comparing T<sub>1</sub>, T<sub>2</sub>, and T<sub>3</sub> processes for ESC and LSC samples reveals that greater activation energies are required for reactions that occurred in the LSC cement clinker. Namely, eggshell powder is more prone to mechanical activation than limestone, so ESC mixtures had higher SSA than limestone mixtures, which in turn increased powder reactivity and, as a result, accelerated the processes that occurred in the ESC cement clinker system during sintering. If the LSC mixture is considered the standard componential mixture for OPC clinker production, it can be established that ESC mixes have a higher sintering rate than OPC, and sintering can be done at a lower temperature.

### CONCLUSIONS

This study looks into the viability of using pulverized eggshell waste instead of limestone to make Portland cement clinker. Overall properties of the synthesized ESC and LSC are evaluated using differential thermal analysis, scanning electron microscopy, and energy dispersive spectroscopy.

The findings of this investigation are summarized as follows:

- Eggshell shows potential as a limestone substitute due to its limestone-like properties, as it is composed of at least 95 % calcium carbonate (CaCO<sub>3</sub>). Mineral phases typical of cement clinker (such as C3S, C2S, C3A, and C4AF) are present both in ESC and LSC mixtures for cement clinker after mechanical activation and sintering at 1300 °C.
- Throughout each stage of the mechanochemical activation, the measured specific surface areas of every investigated sample increased. After initial activation (10 minutes), there was a significant rise in SSA, with samples ESC-1, ESC-2, ESC-3, and ESC-4, showing increases of around 54-55 %. For all eggshell-based samples, there was a 14-16 % change in SSA between 20 and 30 minutes, but only a 20 % difference between 10 and 20 minutes. The LSC sample behaved in a somewhat different way, i.e., after a 60 % initial increase in SSA, there was only 1-2 % variance in SSA during activation. Consequently, compared to traditional limestone cement clinker blends, eggshell-based mixtures activated more readily.
- Given the smaller mean particle size, and thus, higher number of particle interactions, it is reasonable to predict that clinker blends based on eggshells will be more reactive. When ESC-1 and ESC-4 samples are compared, the mixture containing fly ash (ESC-4) yielded the greatest SSA values following varying mechano-activation times, whereas the mixture containing zeolite (ESC-2) came in second.
- According to scanning electron microscopy, most of the grains in the ESC-2 mixture that was mechanically activated for 20 minutes are free, meaning they have not merged into agglomerations. After 30 minutes of mechanical activation, the observed mixture became agglomerated.
- Higher activation energies are needed for reactions that took place in LSC cement clinker, according to a comparison of endothermic processes for ESC and LSC samples. In particular, ESC mixtures exhibited higher SSA than limestone mixtures because of eggshell powder's greater propensity for mechanical activation. This, in turn, increased powder reactivity and accelerated the processes that took place in the ESC cement clinker system during sintering. If the LSC mixture is considered the standard componential mixture for OPC clinker production, it is apparent that ESC mixes have a higher sintering rate than OPC and may be sintered at a lower temperature.

Use of eggshell as a replacement to limestone in cement clinker production can have an environmental impact by minimizing landfill waste and slowing the depletion of primary resources. To make the use of eggshells in cement easier, further research is needed on the industrial-scale regarding synthesis of ESCs by partial replacement of limestone, as well as features of ESC-based mortar and concrete.

### ACKNOWLEDGEMENTS

This investigation is financially supported by the Ministry of Science, Technological Development and Innovation of the Republic of Serbia, NITRA (Contract No.: 451-03-66/2024-03/200012) and Project: 101111694-GREENCO-ERASMUS-EDU-2022-PI-ALL-INNO.

## REFERENCES

- Taylor, H.F.W., Cement Chemistry, 2<sup>nd</sup> Ed., ICE Publishing, 1997. doi: 10.1680/cc.25929
- Schneider, M. (2015), *Process technology for efficient and sustainable cement production*, Cem. Concr. Res. 78(Part A): 14-23. doi: 10.1016/j.cemconres.2015.05.014
- Van Oss, H.G., Padovani, A.C. (2003), *Cement manufacture and the environment Part II: Environmental challenges and opportunities*, J Industr. Ecol. 7(1): 93-126. doi: 10.1162/108819803766729212
- Bernard, E., Rentsch, D., Kuhn, R., et al. (2024), *Earth stabilisation with MgO-based cement*, Cem. Concr. Res. 186: 107655. doi: 10.1016/j.cemconres.2024.107655
- Andrew, R.M. (2019), *Global CO<sub>2</sub> emissions from cement production, 1928-2018*, Earth Syst. Sci. Data, 11(4): 1675-1710. doi: 10.5194/essd-11-1675-2019
- Xue, Z., Zhu, W., Li, L., et al. (2024), *Carbon emissions assessment of cement mixing piles for soft loess improvement and carbon emission reduction using white mud-cement composite material*, Case Stud. Constr. Mater. 21: e03397. doi: 10.1016/j.cscm.2024.e03397
- Cao, H., Han, L., Liu, M., Li, L. (2025), *Spatial differentiation of carbon emissions from energy consumption based on machine learning algorithm: A case study during 2015-2020 in Shaanxi, China*, J Environm. Sci. 149: 358-373. doi: 10.1016/j.jes.2023.08.007
- Kareem, M.A., Ajadi, E.O., Fadipe, O.O., et al. (2025), *Sustainability-driven application of waste steel and tyre rubber fibres as reinforcement in concrete: An optimization study using response surface methodology*, Next Mater. 7: 100345. doi: 10.1016/j.nxmate.2024.100345
- Hanifa, M., Agarwal, R., Sharma, U., et al. (2023), *A review on CO<sub>2</sub> capture and sequestration in the construction industry: Emerging approaches and commercialised technologies*, J CO<sub>2</sub> Utiliz. 67: 102292. doi: 10.1016/j.jcou.2022.102292
- Benhelal, E., Zahedi, G., Shamsaei, E., Bahadori, A. (2013), *Global strategies and potentials to curb CO<sub>2</sub> emissions in cement industry*, J Cleaner Prod. 51: 142-161. doi: 10.1016/j.jclepro.2012.10.049
- Worrell, E., Price, L., Martin, N., et al. (2001), *Carbon dioxide emissions from the global cement industry*, Ann. Rev. Environm. Res. 26: 303-329. doi: 10.1146/annurev.energy.26.1.303
- Atmaca, A., Yumrutaş, R. (2014), *Analysis of the parameters affecting energy consumption of a rotary kiln in cement industry*, Appl. Therm. Eng. 66(1-2): 435-444. doi: 10.1016/j.appltherma.2014.02.038
- Madloul, N.A., Saidur, R., Rahim, N.A., Kamalisarvestani, M. (2013), *An overview of energy savings measures for cement industries*, Renew. Sustain. Energy Rev. 19: 18-29. doi: 10.1016/j.rsener.2012.10.046
- Scrivener, K.L., John, V.M., Gartner, E.M. (2018), *Eco-efficient cements: Potential economically viable solutions for a low-CO<sub>2</sub> cement-based materials industry*, Cem. Concr. Res. 114: 2-26. doi: 10.1016/j.cemconres.2018.03.015
- Mikulčić, H., Klemeš, J.J., Vujanović, M., et al. (2016), *Reducing greenhouse gasses emissions by fostering the deployment of alternative raw materials and energy sources in the cleaner cement manufacturing process*, J Clean. Prod. 136(Part B): 119-132. doi: 10.1016/j.jclepro.2016.04.145
- Terán-Cuadrado, G., Tahir, F., Nurdawati, A., et al. (2024), *Current and potential materials for the low-carbon cement production: Life cycle assessment perspective*, J Build. Eng. 96: 110528. doi: 10.1016/j.job.2024.110528
- Schneider, M., Romer, M., Tschudin, M., Bolio, H. (2011), *Sustainable cement production-present and future*, Cem. Concr. Res. 41(7): 642-650. doi: 10.1016/j.cemconres.2011.03.019
- Sathiparan, N., De Zoysa, H.T.S.M. (2018), *The effects of using agricultural waste as partial substitute for sand in cement blocks*, J Build. Eng. 19: 216-227. doi: 10.1016/j.job.2018.04.023
- Son, Y., Yang, J., Kim, W., Park, W. (2024), *Advanced bacteria-based biomaterials for environmental applications*, Biore-source Technol. 414: 131646. doi: 10.1016/j.biortech.2024.131646
- Hamada, H.M., Tayeh, B.A., Al-Attar, A., et al. (2020), *The present state of the use of eggshell powder in concrete: A review*, J Build. Eng. 32: 101583. doi: 10.1016/j.job.2020.101583
- Faure, A., Coudray, C., Anger, B., et al. (2019), *Beneficial reuse of dam fine sediments as clinker raw material*, Constr. Build. Mater. 218: 365-384. doi: 10.1016/j.conbuildmat.2019.05.047
- Mansour, S.M. (2021), *Use of natural pyrophyllite as cement substitution in ultra performance polypropylene fiber concrete*, Int. J Eng. Res. Africa, 56: 123-135. doi: 10.4028/www.scientific.net/JERA.56.123
- Puertas, F., Garcia-Diaz, I., Barba, A., et al. (2008), *Ceramic wastes as alternative raw materials for Portland cement clinker production*, Cem. Concr. Compos. 30(9): 798-805. doi: 10.1016/j.cemconcomp.2008.06.003
- Tsakiridis, P.E., Agatzini-Leonardou, S., Oustadakis, P. (2004), *Red mud addition in the raw meal for the production of Portland cement clinker*, J Hazard. Mater. 116(1-2): 103-110. doi: 10.1016/j.jhazmat.2004.08.002
- Canpolat, F., Yilmaz, K., Köse, M.M., et al. (2004), *Use of zeolite, coal bottom ash and fly ash as replacement materials in cement production*, Cem. Concr. Res. 34(5): 731-735. doi: 10.1016/S0008-8846(03)00063-2
- Young, G., Yang, M. (2019), *Preparation and characterization of Portland cement clinker from iron ore tailings*, Constr. Build. Mater. 197: 152-156. doi: 10.1016/j.conbuildmat.2018.11.236
- Lin, K.-L., Lo, K.-W., Hung, M.-J., et al. (2018), *Utilization of reduction slag and waste sludge for Portland cement clinker production*, Environm. Prog. Sustain. Energy, 37(2): 669-677. doi: 10.1002/ep.12736
- Her, S., Park, T., Zalnezhad, E., Bae, S. (2021), *Synthesis and characterization of cement clinker using recycled pulverized oyster and scallop shell as limestone substitutes*, J Clean. Prod. 278: 123987. doi: 10.1016/j.jclepro.2020.123987
- Kirgiz, M.S. (2015), *Use of ultrafine marble and brick particles as raw materials in cement manufacturing*, Mater. Struct. 48: 2929-2941. doi: 10.1617/s11527-014-0368-6
- Chen, I.A., Juenger, M.C. (2009), *Incorporation of waste materials into portland cement clinker synthesized from natural raw materials*, J Mater. Sci. 44(10): 2617-2627. doi: 10.1007/s10853-009-3342-x
- Jittin, V., Bahurudeen, A., Ajinkya, S.D. (2020), *Utilisation of rice husk ash for cleaner production of different construction products*, J Cleaner Prod. 263: 121578. doi: 10.1016/j.jclepro.2020.121578
- Chowdhury, S., Mishra, M., Suganya, O. (2015), *The incorporation of wood waste ash as a partial cement replacement material for making structural grade concrete: An overview*, Ain Shams Eng. J, 6(2): 429-437. doi: 10.1016/j.asej.2014.11.005
- Bahurudeen, A., Kanraj, D., Dev, V.G., Santhanam, M. (2015), *Performance evaluation of sugarcane bagasse ash blended cement in concrete*, Cem. Concr. Compos. 59: 77-88. doi: 10.1016/j.cemconcomp.2015.03.004



34. Li, G., Xu, X., Chen, E., et al. (2015), *Properties of cement-based bricks with oyster-shells ash*, J Clean. Product. 91: 279-287. doi: 10.1016/j.jclepro.2014.12.023
35. Faridi, H., Arabhosseini, A. (2018), *Application of eggshell wastes as valuable and utilizable products: A review*, Res. Agr. Eng. 64(2): 104-114. doi: 10.17221/6/2017-RAE
36. Baláz, M. (2018), *Ball milling of eggshell waste as a green and sustainable approach: A review*, Adv. Coll. Interf. Sci. 256: 256-275. doi: 10.1016/j.cis.2018.04.001
37. Intharapat, P., Kongnoo, A., Kateungngan, K. (2013), *The potential of chicken eggshell waste as a bio-filler filled epoxidized natural rubber (ENR) composite and its properties*, J Polym. Environ. 21(1): 245-258. doi: 10.1007/s10924-012-0475-9
38. Oliveira, D.A., Benelli, P., Amante, E.R. (2013), *A literature review on adding value to solid residues: egg shells*, J Cleaner Prod. 46: 42-47. doi: 10.1016/j.jclepro.2012.09.045
39. Lee, S.J., Oh, S.H. (2003), *Fabrication of calcium phosphate bioceramics by using eggshell and phosphoric acid*, Mater. Lett. 57(29): 4570-4574. doi: 10.1016/S0167-577X(03)00363-X
40. Pradhan, A.K., Sahoo, P.K. (2017), *Synthesis and study of thermal, mechanical and biodegradation properties of chitosan-g-PMMA with chicken egg shell (nano-CaO) as a novel bio-filler*, Mater. Sci. Eng. C Mater. Biol. Appl. 80: 149-155. doi: 10.1016/j.msec.2017.04.076
41. Juan, Y.K., Lai, W.Y., Shih, S.G. (2017), *Building information modeling acceptance and readiness assessment in Taiwanese architectural firms*, J Civ. Eng. Manag. 23(3): 356-367. doi: 10.3846/13923730.2015.1128480
42. Celik, K., Jackson, M.D., Mancio, M., et al. (2014), *High-volume natural volcanic pozzolan and limestone powder as partial replacements for portland cement in self-compacting and sustainable concrete*, Cem. Concr. Compos. 45: 136-147. doi: 10.1016/j.cemconcomp.2013.09.003
43. De Weerd, K., Ben Haha, M., Le Saout, G., et al. (2011), *Hydration mechanisms of ternary Portland cements containing limestone powder and fly ash*, Cem. Concr. Res. 41(3): 279-291. doi: 10.1016/j.cemconres.2010.11.014
44. Binici, H., Aksogan, O., Sevinc, A.H., Cinpolat, E. (2015), *Mechanical and radioactivity shielding performances of mortars made with cement, sand and egg shells*, Constr. Build. Mater. 93: 1145-1150. doi: 10.1016/j.conbuildmat.2015.05.020
45. Pliya, P., Cree, D. (2015), *Limestone derived eggshell powder as a replacement in Portland cement mortar*, Constr. Build. Mater. 95: 1-9. doi: 10.1016/j.conbuildmat.2015.07.103
46. Zain, M.R.M., Oh, C.L., Lee, S.W. (2021), *Investigations on rheological and mechanical properties of self-compacting concrete (SCC) containing 0.6  $\mu\text{m}$  eggshell as partial replacement of cement*, Constr. Build. Mater. 303: 124539. doi: 10.1016/j.conbuildmat.2021.124539
47. Her, S., Park, J., Li, P., Bae, S. (2022), *Feasibility study on utilization of pulverized eggshell waste as an alternative to limestone in raw materials for Portland cement clinker production*, Constr. Build. Mater. 324: 126589. doi: 10.1016/j.conbuildmat.2022.126589
48. Terzić, A., Pezo, L., Miličić, Lj., et al. (2019), *Thermal and mechanical behavior of composite mortars containing natural sorptive clays and fly ash*, Sci. Sinter. 51(1): 39-56. doi: 10.2298/SOS1901039T
49. Terzić, A., Pezo, L., Mijatović, N., et al. (2018), *The effect of alternations in mineral additives (zeolite, bentonite, fly ash) on physico-chemical behavior of Portland cement based binders*, Constr. Build. Mater. 180: 199-210. doi: 10.1016/j.conbuildmat.2018.06.007
50. Terzić, A., Radulović, D., Pezo, L., et al. (2017), *The effect of mechano-chemical activation and surface treatment of limestone filler on the properties of construction composites*, Compos. Part B: Eng. 117: 61-73. doi: 10.1016/j.compositesb.2017.02.041
51. Blaine, R.L., Kissinger, H.E. (2012), *Homer Kissinger and the Kissinger equation*, Thermoch. Acta. 540: 1-6. doi: 10.1016/j.tca.2012.04.008
52. Chen, D. Gao, X., Dollimore, D. (1993), *A generalized form of the Kissinger equation*, Thermoch. Acta, 215: 109-117. doi: 10.1016/0040-6031(93)80085-O
53. Terzić, A., Obradović, N., Andrić, Lj., et al. (2015), *Investigation of thermally induced processes in corundum refractory concretes with addition of fly ash*, J Therm. Anal. Calorim. 119: 1339-1352. doi: 10.1007/s10973-014-4230-4
54. Kissinger, H.E. (1957), *Reaction kinetics in differential thermal analysis*, Anal. Chem. 29(11): 1702-1706. doi: 10.1021/ac60131a045
55. Xu, W., Xu, J., Liu, J., et al. (2014), *The utilization of lime-dried sludge as resource for producing cement*, J Clean. Product. 83: 286-293. doi: 10.1016/j.jclepro.2014.07.070
56. Chen, X., Li, J., Lu, Z., et al. (2022), *The role of brownmillerite in preparation of high-belite sulfoaluminate cement clinker*, Appl. Sci. 12(10): 4980. doi: 10.3390/app12104980

© 2024 The Author. Structural Integrity and Life, Published by DIVK (The Society for Structural Integrity and Life 'Prof. Dr Stojan Sedmak') (<http://divk.inovacionicentar.rs/ivk/home.html>). This is an open access article distributed under the terms and conditions of the [Creative Commons Attribution-NonCommercial-NoDerivatives 4.0 International License](https://creativecommons.org/licenses/by-nc-nd/4.0/)